Heat transfer modeling for turbocharger control

Josefin Storm

LINKÖPING UNIVERSITY

Master of Science Thesis in Electrical Engineering

Heat transfer modeling for turbocharger control

Josefin Storm

LiTH-ISY-EX--17/5098--SE

Supervisor: **Kristoffer Ekberg**
                 ISY, Linköping University
                 Patrik Martinsson
                 Volvo Car Corporation

Examiner: **Lars Eriksson**
                 ISY, Linköpings University

Division of Automatic Control
Department of Electrical Engineering
Linköping University
SE-581 83 Linköping, Sweden

Abstract

Turbocharging is a way to stay competitive on the market where there are increasing demands on fuel consumption and engine performance. Turbocharging lets the engine work closer to its maximum power and thereby reduces the relative losses due to pumping and friction. The turbocharger is exposed to big temperature differences and heat flows will occur both internally between the turbine and the compressor as well as between the turbocharger and its surroundings. A way to get a better understanding of the behaviour of the turbocharger is to understand the heat flows better. This thesis is therefore aimed at investigating the effect of heat transfer on the turbocharger. In the thesis, different ways of account for the heat transfer within the turbocharger is investigated and a heat transfer model is presented and validated. The model can be used as a tool to estimate the importance of different heat flows within the turbocharger. A set of heat transfer coefficients are estimated and the heat transfer is modelled with good accuracy for high engine loads and speeds.

Acknowledgement

I would like to thank my examiner Lars Eriksson and Volvo Cars for giving me the opportunity to write this thesis.

I would also like to thank my supervisors at Linköping University and Volvo Cars for all support and guidance. A special thank to Patrik Martinsson at Volvo Cars for helping out whenever I had questions, and to Kristoffer Ekberg at Linköping University for your patience and for that the door to your office was always open when I ran into problems or had questions about the work.

Finally I would like to thank my family for the support and encouragement during my thesis work and throughout life. Thank you.

Contents

Notation	Definition
A	Area $[m^2]$
Bi	Biot number [-]
c_p	Specific heat capacity $[J/kgK]$
D	Pipe inner diameter $[m]$
g	Gravitational constant $[m/s^2]$
Gr	Grashof's number [-]
h	Heat transfer coefficient $[W/m^2K]$
k	Thermal conductivity $[W/mK]$
l	Pipe length $[m]$
L	Characteristic length $[m]$
m	Mass $[kg]$
M	Mach number turbine [-]
$\dot{m}$	Mass flow $[kg/s]$
p	Pressure $[Pa]$
Pr	Prandtl's number [-]
Pr	Pressure ratio [-]
R	Specific gas constant $[J/kgK]$
Re	Reynold's number [-]
Nu	Nusseldt's number [-]
$\dot{Q}$	Heat flow $[W]$
T	Temperature $[K]$
V	Volume $[m^2]$
vel	Velocity $[m/s]$
$\dot{W}$	Power $[W]$
β	Parameter $[1/K]$
γ	Specific heat capacity ratio [-]
ϵ	Emissivity [-]
η	Efficiency [-]
μ	Dynamic viscosity $[kg/ms]$
ν	Kinematic viscosity $[m^2/s]$
σ	Stefan-Boltzmann constant $[W/m^2K^4]$

Notation	Definition
01	Compressor inlet
02	Compressor outlet
03	Turbine inlet
04	Turbine outlet
air	Intake air
amb	Ambient
m, in	Exhaust manifold inlet
m, out	Exhaust manifold outlet
bh	Bearing housing
c	Compressor
cat	Catalyst
$cond$	Conduction
$conv$	Convection
exh	Exhaust gas
in	inlet, inside
L	Mean value over characteristic length
oil	Oil
out	Outlet, outside
rad	Radiation
t	Turbine
t, sol	Turbine housing
w	Exhaust manifold wall

1

Introduction

1.1 Problem Formulation

Downsizing of combustion engines is today a common way to achieve a lower fuel consumption and stay competitive on a market where fuel economy has become more important. [14] While downsizing lowers the losses it also lowers the maximum power output from the engine. The amount of air in the cylinders is critical for combustion and through turbocharging the density of the intake air can be increased enabling a higher power output from the downsized engine. By using a turbocharger a compromise can be made between low fuel consumption and power output.

The turbocharger is exposed to several heat flows, driven by temperature differences between the working fluids of the turbine and the compressor, as well as the temperature difference between high and low-pressure side [7]. The heat transfer affects the efficiency of the turbocharger which is normally calculated from fluid temperatures and pressures [14]. This can lead to a calculated efficiency that is either under- or overestimated. Heat transfer may increase the compressor outlet temperature giving a higher estimation of the power consumed by the compressor leading to a lower calculated compressor efficiency. A decrease in turbine outlet temperature due to heat transfer gives a higher estimation of the turbine power which leads to an increase in calculated turbine efficiency.

With increasing demands on reduced fuel consumption, emissions and driving experience, more precise models are wanted for improved control. A heat transfer model for the turbocharger giving a better estimation of fluid temperatures could be one step towards better control. The main purpose of this thesis is to find and implement a model for the heat transfer between the exhaust gas, the turbine housing and its surroundings to improve the estimations of turbine outlet temperature.

1.2   Purpose and goal

The objectives of the thesis are to investigate the heat transfers affecting the turbocharger. The knowledge about the heat transfer could be used to improve turbo control model with potential to improve driveability and performance. The main purpose of the thesis will be to find models that describe the heat transfer between the turbine and its surroundings to get a better estimation of turbine inlet and outlet temperature. Matlab is used for developing estimation algorithms for the heat transfer effects and the models are validated in a suitable manner.

1.3   Delimitations

The project is limited to only investigate the heat transfer effects on one specific turbocharger connected to one specific engine. All results will therefore be concerning this specific turbocharger and will not be general. However, it should be easy to parametrize other turbochargers like the one used during the project by repeating the same measurements. All measurements will be made in an engine test rig. The turbocharger used is a double turbocharger which will be treated as a single step turbocharger as far as possible. For example, the mass flow through the small turbocharger will be kept to a minimum. The project does not include to implement the models in a complete mean value engine model, even though that could be done in the future.

1.4   Outline

A short description of the outline of the thesis is described here.
Chapter 1, Introduction
Introduction with background, problem formulation, purpose and delimitations.
Chapter 2, Related research
Theory and related research needed to understand the problem.
Chapter 3, Models
Overview of the system as well as descriptions of the models used.
Chapter 4, Measurements
Test setup and description on how measurements were conducted.
Chapter 5, Implementation
How the models were implemented.
Chapter 6, Result
Result and a short analysis of the result.
Chapter 7, Discussion
Discussion of the process and the obtained result.
Chapter 8, Conclusion
Conclusion and suggestions on future work.

2

Related research

2.1 Turbocharging

A turbocharger consists of a compressor connected to a turbine through a shaft
[14]. The compressor compresses the air before going to the intake manifold
leading to a higher pressure and temperature. The air passes an intercooler to
lower the temperature before going into the cylinders. The exhaust gas passes the
turbine where the enthalpy change drives the shaft connected to the compressor.
Thereafter the exhaust gas passes through the exhaust system with a catalyst.
Figure 2.1 shows a schematic of an SI engine with a turbocharger.
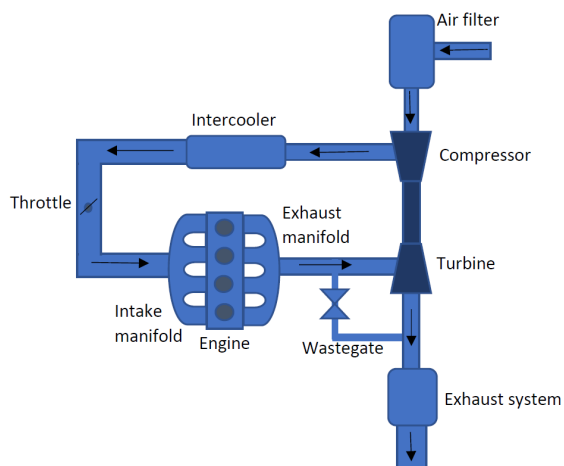
Figure 2.1: SI-engine with turbocharging

Higher pressure on the intake air gives a higher amount of oxygen to the cylinders and more fuel can be combusted. A turbocharged engine manage to burn more fuel than a naturally aspirated engine of the same size enabling a higher power output. If a smaller turbocharged engine is compared to a bigger naturally aspirated engine while cruising the turbocharged engine works closer to its maximum torque. The relative losses due to pump work and friction will be smaller while the smaller engine has less margin to its maximum torque affecting the ability to accelerate. During combustion all energy cannot be used and through turbocharging can parts of the energy lost in the thermodynamic cycle be reused. To get a better low speed torque a small turbocharger is preferable while it lowers the maximum engine power. One way to get around this tradeoff is to introduce double stage turbocharging. Two different turbochargers can then be connected either in series or in parallel. By using two different sizes of turbochargers it is possible to alter between them depending on need. For low engine speed the smaller is used while it is bypassed for high speeds.

A common way to include the turbochargers in the engine simulation code is to interpolate the efficiency and flow maps. Since the working region of the turbocharger often exceeds the regions covered in the maps extrapolation is often used.

2.2   First law of thermodynamics

The first law of thermodynamics states that "energy can be neither created nor destroyed during a process; it can only change forms" [9]. Energy can be transferred in forms of heat transfer, Q, work transfer, W, or mass flow, $\dot{m}$. [9], [29]. For a system where the states do not change during the process the total energy change is zero.

For a closed system the first law of thermodynamics can be written as in Equation 2.1 if there is no change in potential or kinetic energy.

$$mc_v \frac{dT}{dt} = (\dot{Q}_{in} - \dot{Q}_{out}) + (\dot{W}_{in} - \dot{W}_{out}) \tag{2.1}$$

where $mc_v \frac{dT}{dt}$ is the change in internal energy. This is zero if there is no temperature change. m is the thermal mass and c_v is the heat capacity of the material. $\dot{Q}$ is the heat flow and $\dot{W}$ is the work transfer.

For an open system with stationary flow the first law of thermodynamics can be expressed as in 2.2 if there is no change of kinetic or potential energy.

$$\dot{m}c_p(T_{out} - T_{in}) = (\dot{Q}_{in} - \dot{Q}_{out}) + (\dot{W}_{in} - \dot{W}_{out}) \tag{2.2}$$

Where $\dot{m}$ is the mass flow, c_p the specific heat capacity, T is the temperature, $\dot{Q}$ heat flow $\dot{W}$ the work transfer.

2.3   Heat transfer

During heat transfer energy is transferred from a warm medium to a colder one
and the temperature difference is driving the process [9]. The temperature has
a big impact on the heat flux [29]. Heat transfer can be divided into conduction,
convection and radiation.

2.3.1   Conduction

Conduction is heat transfer within solids, fluids and gases [9]. Geometry, material
and temperature difference affect the rate of heat conduction. The thermal con-
ductivity of a material, k, describes how well the material conducts heat. There
is often a connection between thermal and electric conductivity. For heat con-
duction in one direction can Fourier's law of heat conduction be used [27]. The
one-dimensional form is described in Equation 2.3.

$$\dot{Q}_{cond} = kA\frac{dT}{dx} \tag{2.3}$$

$\dot{Q}_{cond}$ is the heat conduction which can be determined by the thermal conduc-
tivity, k, the area across heat flow, A, and the temperature gradient $\frac{dT}{dx}$.

2.3.2   Convection

Convection which is heat transfer between a fluid in motion and a solid can be
either natural or forced [9]. Natural convection is induced by shifting in density
depending on temperature while forced convection is when the fluid is moved by
an external force. The convection can be described by Equation 2.4 [27].

$$\dot{Q}_{conv} = hA\Delta T \tag{2.4}$$

The convective heat flow, $\dot{Q}_{conv}$, is determined by the area where the heat is
transferred, A, the temperature differences between the solid and the surround-
ing fluid, ΔT, and the convection heat transfer coefficient, h.

The heat transfer coefficient h is normally a function depending on the flow
conditions, the surface geometry, the properties of the fluid, the bulk fluid ve-
locity and the temperature difference between solid and surrounding [29], [9].
In general, the heat transfer coefficient varies along the flow direction. The ve-
locity has a big impact on the heat transfer coefficient, a higher velocity gives a
higher heat transfer coefficient. Typical heat transfer coefficients for gases are
2-25 W/m^2K for free convection and 25-250 W/m^2K for forced convection.

2.3.3   Radiation

Heat can also be transferred through radiation which becomes more significant
at high temperatures [19]. Heat transfer from a surface can be described by Equa-
tion 2.5 [29].

$$\dot{Q}_{rad} = \sigma \epsilon A T^4 \tag{2.5}$$

$\sigma = 5.67 \cdot 10^{-8}$ is the Stefan-Boltzmann constant, T is the temperature of the object, A is the area and ϵ is the emissivity which has a value between 0 and 1.

The heat transfer between two surfaces can be described by Equation 2.6. The emissivity ϵ_{12} depends on the emissivity of the two objects as well as the geometry.

$$\dot{Q}_{rad} = \epsilon_{12} \sigma A_1 (T_1^4 - T_2^4) \tag{2.6}$$

A_1 and T_1 is the area and temperature of the radiating body, and T_2 is the temperature of the surrounding surface.

The heat flux caused by radiation can be linearized giving the radiation heat flux according to 2.7.

$$\dot{Q}_{rad} = h_s A (T_1 - T_2) \tag{2.7}$$

2.4   State-of-the-art

This section investigates previously done studies within the field. The focus is on turbocharger heat transfer and investigation in one-dimensional models including heat transfer but there is also a section concerning temperature drop in the exhaust manifold.

2.4.1   Turbocharger heat transfer

On the compressor side heat is often transferred from the housing to the gas [14]. This leads to a higher temperature in the compressor which in turn decreases the calculated compressor efficiency. Heat transfer may also occur from the hot gases to the pipes after the compressor which could increase the calculated compressor efficiency. The heat transfer in the turbine however is more significant and due to the high temperature differences the heat is transferred to the surroundings of the turbine, the bearing housing and the compressor. The heat transfer has a bigger impact on the performance of the turbine compared to the compressor .

In Sirakov and Casey [28] it is noted that the heat flow between compressor and turbine increases the power consumption of the compressor leading to lower efficiency. Since the compressor power is used to derive the turbine power and efficiency, the turbine efficiency increases. This means that the turbine gets an overestimated efficiency and the compressor an underestimated efficiency. This is is shown more prominent for low mass flows and low rotational speeds [28], [30].

In Baines et al. [4] it is shown that the internal heat transfer from the turbine to the bearing housing as well as the external heat transfer from the turbine to the environment are the most important for the turbocharger performance.

In Payari et al. [21] consideration is taken to radiation and convective heat transfer in a simplified external heat transfer model. Here it is concluded that

the source that has the biggest external heat fluxes is the surface of the turbine. The reason for this is its big areas and high temperatures. In comparison is the external heat fluxes in the central housing insignificant. The running conditions determine whether heat is absorbed or lost on the compressor side. Here the radiated heat from the turbine appear to be of biggest importance even though other ways of heat transfer cannot be ignored. However, in Bohn et al. [6] it is said that heat radiation has a small impact on the total heat flux between the turbine and the compressor due to the turbocharger geometry.

In Aghaali et al. [2] an analytic and experimental work to compare different methods of heat transfer modelling is presented. By altering the heat transfer conditions with respect to conduction, convection and radiation they show that altering convective heat transfer conditions has the biggest impact on the heat fluxes.

In Burke et al. [7] an investigation was made on whether the heat transfer should be divided into pre-and post-compression heat transfer, showing that for low speeds the assumption that all heat transfer occurs at the high temperature, high pressure side is valid.

The state of the art regarding turbocharger heat transfer was used as support when determining which heat flows to include in the model. It was also used as a comparison when evaluating the results.

2.4.2   One-dimensional heat transfer models

In several works [25], [24], [26], [20], [22] ways to model the heat transfer through lumped capacity models are presented and discussed. The model developed in this thesis was inspired from these works and builds upon the method of lumped capacitance. These models can be used to correct the turbocharger performance maps which are used to predict the behaviour of the turbochargers. Correction of the maps increase the accuracy when the maps are used in operation points different to the one when the measurements for the map was made.

In Cormerais et. al. [10] an experimental characterization was performed to determine the heat transfer coefficients. Thereafter they used the equivalent heat transfer resistance method to calculate internal and external heat transfer during steady and transient conditions. The method was evaluated through comparisons between numerical and experimental results. Different types of tests were performed where the turbocharger adiabatic, non-adiabatic and transient behaviour could be studied. The method showed on good ability to model the heat transfer correctly, both internal and external, however the result is not totally agreeing with measurements for transient conditions.

In Romagnoli and Martinez-Botas [22] it was found that there is a linear relationship between the temperatures of the exhaust gas and the surface temperature of the compressor and turbine. In Aghali and Ångström [1] a procedure of determining the turbine outlet temperature from turbine inlet temperature is described. This way of modelling was also considered through this thesis, but with less focus than the lumped capacitance model since this method cannot differentiate between different heat flows.

In Tanda et al. [30] the possibilities to use an infrared thermography and the Fourier conduction law to evaluate the heat transfer rate from the turbine to the compressor is investigated and a correction model for the measured diabatic efficiency is presented. A thermodynamic analysis of the turbocharger is made by comparing an isotropic adiabatic process and a diabatic non-ideal process. An adiabatic non-ideal process is achieved by minimizing the internal and external heat transfer and the shaft power is assumed to be equal to the enthalpy drop. In the diabatic case the enthalpy change can be seen as the sum of work and heat transfer rates. This study was a good inspiration for the suggestions of future work given in this thesis.

In Sirakov and Casey [28] a correction model that converts the diabatic performance maps to maps for adiabatic conditions for both compressor and turbine is defined, using a simplified method compared to the method in Casey and Feish [8]. In Marelli et al. [17] a correction model for compressor maps is presented. Even though this correction model uses a simplified geometry, experimental tests show that the suggested model makes it possible to evaluate the adiabatic performances of a compressor with good precision. This work shows that a good result can be accomplished even with a simplified geometry, something that was also accompished in this thesis.

In Marelli [18] the influence of internal heat transfer on turbine thermochemical efficiency was investigated. The proposed solution suggests models for corrected performance maps of the turbocharger. A comparison with quasi-adiabatic curves shows good agreement.

2.4.3   Exhaust manifold temperatures

In Eriksson [13] three different ways to model the exhaust manifold temperature is discussed. All are lumped parameter heat transfer models and are intended to be used in mean value engine models. The models are based on temperature drop in straight pipes, outlet temperature from the engine and different heat transfer modes. To model the temperature drop in the exhaust manifold is important since the performance of the turbocharger and catalyst depend on the exhaust gas temperature. It is also stated that the conduction into the engine block should be considered in the models. Heat transfer coefficients can be modelled with Reynolds number and Prandtl number but can also be assumed to be constant, however this can lead to an underestimation of heat transfer at high flows as well as an overestimation of heat transfer for low flows. Arguments for modelling the wall temperature as constant is presented and measurements show that the wall temperature does not show an exponential decay along the pipe. This work was a big inspiration for the modelling of the exhaust manifold temperatures.

In [16] a dual wall exhaust manifold was modelled. It is stated that cast iron exhaust manifolds absorb a high amount of energy during cold start due to its high thermal capacity. The dual wall exhaust manifold on the other hand has a lower thermal capacity and a better isolating effect.

3

Models

3.1 System overview

The system studied is a double turbo charger consisting of two turbochargers of different size. Each turbocharger consists of a centrifugal compressor and a radial turbine connected with a shaft. The shaft is lubricated with oil which also works as a coolant. Measurements and modelling were only made on the bigger turbocharger. The flow through the smaller was kept as small as possible without risk of malfunction. The heat transfer and mass flow through the smaller turbocharger were ignored in the models. The energy flows of one of the turbochargers is shown in Figure 3.1. The main energy flows considered are the mass flows into and out from the compressor and turbine, the mechanical power transferred through the shaft from the turbine to the compressor but also losses in form of internal and external heat transfer. Due to the engine work cycle the flow is pulsating, however for modelling only a mean value model was considered.
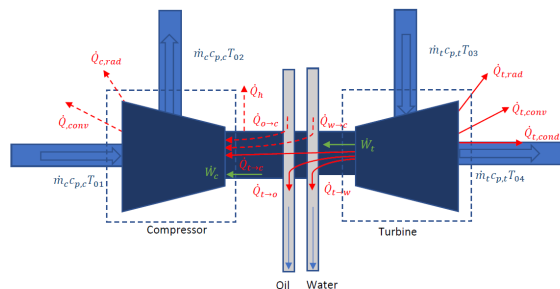
Figure 3.1: Energy flows to and from the compressor and the turbocharger

3.2   Temperature change over turbine

Two different approaches were used to model the turbocharger to include the heat transfer effects. The first model is a physically based model while the second method uses an experimental characterization to determine different coefficients and from this determine the turbine outlet temperature from the turbine inlet temperature and the oil inlet temperature. The later could not be evaluated due to lack of measurements on bearing housing and oil inlet temperatures. An attempt to use other measurements instead was made but did not work and that method is therefore described in Appendix A.

The first method developed is built upon the method of lumped capacities as described in [5]. Systems with a relatively small temperature gradient can be described by a lumped heat capacity model for unsteady conduction[15]. An idealization is made that the temperature distribution over the object is uniform and it can be used for describing transient behaviour. In general, it can be said that the smaller the object, the more correct is this method for describing reality. For a lumped capacity analysis, it is assumed that the internal resistance of the object is negligible compared to the external resistance. The Biot number compares the relative size of the internal and external heat transfer. The Biot Bi, number is described in equation 3.1 where V is the volume of the body, A is the area exposed to convection, h describes the convection and k the internal conduction [29]. The lumped capacitance method is only valid if $Bi < 0.1$.

$$Bi = \frac{hV}{kA} \tag{3.1}$$

The model looks slightly different depending on if it is aimed for static or transient use. Both models are described below but only the static model was implemented.

3.2.1   Static model

The turbine was divided into two control volumes, one for the gas and one for the solid part. The first law of thermodynamics was applied to these volumes giving two equations with relationships between temperatures. The heat transfer coefficients were estimated during steady state operation for one control volume at a time with the method of least squares. The two equations describing the model can be combined and the turbine outlet temperature can then be determined from turbine inlet temperatures.

Gas control volume, heat transfer coefficient inside

The control volume of the gas describes the gas inside the turbine where enthalpy change in the gas drives the turbocharger shaft. The energy flows of the gas control volume is illustrated in Figure 3.2. The energy flows considered are the mass flows in and out from the turbine, the work transfer to the compressor, the heat transfer to the turbine housing and friction losses in the bearing housing.
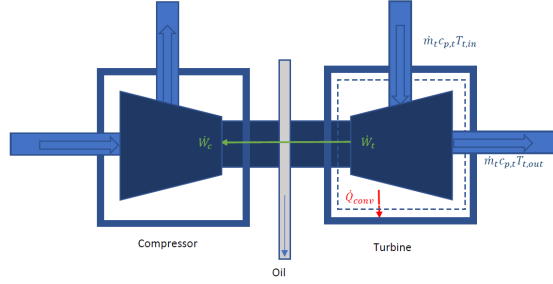
Figure 3.2: *Energy flows connected to the gas control volume. The dashed lines illustrate the boundaries of the control volume.*

Application of the first law of thermodynamics on the control volume for the gas gave Equation 3.2. Convection was assumed to occur with a uniform temperature even though there is a temperature drop over the turbine. The enthalpy change in the exhaust gases is assumed to be transformed into mechanical work used by the compressor and to friction as well as heat transfer to the turbine housing. The mass flow is assumed to be the same for inlet and outlet gases.

$$\dot{m}_{exh}c_{p,exh}(T_{t,in} - T_{t,out}) = h_{t,in}A_{t,in}(T_g - T_{t,sol}) + \dot{W}_t \qquad (3.2)$$

$\dot{m}_{exh}$ and $c_{p,exh}$ is the mass flow and the specific heat capacity of the exhaust gas respectively. $T_{t,in}$ and $T_{t,out}$ describes the inlet and outlet temperature of the exhaust gas and $A_{t,in}$ is the area where heat transfer was assumed to happen, estimated from CAD-models. $T_{t,sol}$ is the mean housing temperature of the turbine housing. $h_{t,in}$ is the heat transfer coefficient which was estimated from measurements through curve fitting with least square method. Different values on T_g was used to find the best fit. The work $\dot{W}_t$ is estimated from the work used by the compressor as described in Equation 3.3.

$$\dot{W}_c = \dot{m}_{air}c_{p,air}(T_{c,out} - T_{c,in}) \qquad (3.3)$$

In reality will it occur heat transfer even here but due to lower temperatures it was neglected. The work from the turbine $\dot{W}_t$ will be used to drive the compressor and some will be lost due to friction giving $\dot{W}_t \approx \dot{W}_c + \dot{W}_{fric}$. In the first iteration was the friction losses ignored.

Solid control volume, heat transfer coefficient outside

By introducing a control volume including the solid part of the turbine housing and applying the first law of thermodynamics Equation 3.4 was obtained. The energy flows considered are the convective heat transfers on the inside and the outside of the turbine, the radiation to the surroundings as well as the conduction to the connecting solid parts. The energy flows are illustrated in Figure 3.3
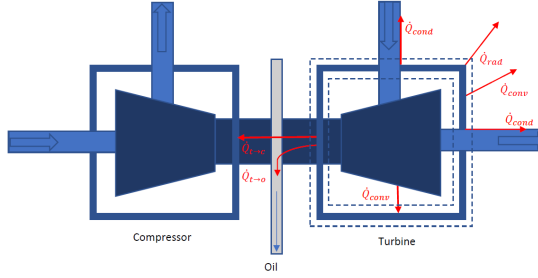
Figure 3.3: *Energy flows connected to the solid control volume of the turbine. The dashed lines illustrate the boundaries of the control volume.*

$$
\begin{aligned}
0 =& h_{t,in}A_{t,in}(T_g - T_{t,sol}) - h_{t,out}A_{t,out}(T_{t,sol} - T_{amb}) - \\
& \epsilon_t \sigma A_{t,out}(T_{t,sol}^4 - T_{amb}^4) - \dot{m}_{oil}c_{p,oil}(T_{oil_{in}} - T_{oil,out}) - \\
& k_{t-cat}A_{t-cat}\frac{dT_{t-cat}}{dx} - k_{exh-t}A_{exh-t}\frac{dT_{exh-t}}{dx} - k_h A_h \frac{dT_h}{dx}
\end{aligned}
\tag{3.4}
$$

$h_{t,in}$ and $h_{t,out}$ are the inside and outside heat transfer coefficients, $A_{t,in}$ and $A_{t,out}$ are the inside and outside areas of the turbocharger where heat transfer occur. T_g is the gas temperature on the turbine inside, $T_{t,sol}$ is the housing temperature of the turbine and T_{amb} is the ambient temperature. ϵ_t is the emissivity and σ the Stefan-Boltzmann constant. $\dot{m}_{oil}$ is the oil mass flow, $c_{p,oil}$ the specific heat capacity of the oil, $T_{oil_{in}}$ the oil temperature before the bearing housing and $T_{oil,out}$ the oil temperature after the bearing housing. k_{t-cat} is the conductivity of the material between turbine and catalyst, A_{t-cat} the connecting area and $\frac{dT_{t-cat}}{dx}$ is the heat transfer rate. k_{exh-t} is the conductivity of the material between the turbine and the exhaust manifold, A_{exh-t} the connecting area and $\frac{dT_{exh-t}}{dx}$ the heat transfer rate. k_h is the conductivity of the bearing housing, A_h its cross area and $\frac{dT_h}{dx}$ the heat transfer rate over it.

The first term on the right side describes the convective heat transfer between the exhaust gas and the turbine housing and the second term is the convective heat transfer from the turbine housing to the surrounding air. The third term describes the radiation heat transfer to the surrounding and the next is the energy transferred to the oil. The last three terms describe the conduction heat transfer to the connecting parts. Conductive heat transfer occurs between the turbine housing and the catalyst, the exhaust manifold and the bearing housing towards the compressor. The heat transfer from turbine to compressor consist of convection, radiation and conduction, however the radiation and convection between the turbine and compressor were being neglected. The heat transfer rate $\frac{dT}{dx}$ was intended to be estimated as the temperature difference between two surface temperatures divided by the perpendicular distance between the measurement points. However, the conductivity showed to be difficult to estimate, how this was handled is described in Chapter 5.

    The heat transfer coefficient $h_{t,out}$ and the emissivity ϵ_t was determined through curve fitting with least square method. By combining Equation 3.2 and 3.4 can the outlet temperature of the turbine be determined from turbine inlet temperature.

3.2.2   Dynamic model

For the dynamic model are the constants $h_{t,in}$, $h_{t,out}$ and ϵ_t estimated in Section 3.2.1 needed. Since the temperature change in the gas happens almost immediate compared to the temperature change in the solid is Equation 3.2 used for the dynamic model as well. The equation for the solid part is extended to include the change of the internal energy in the material and is for the dynamic model described with Equation 3.5.

$$m_{t,sol} c_{v,t} \frac{d T_{t,sol}}{dt} = \dot{Q} \tag{3.5}$$

    Where $m_{t,sol}$ is the mass of the turbine housing, c_v is the heat capacity of the housing material, $\frac{d T_{t,sol}}{dt}$ is the temperature change and $\dot{Q}$ the heat transfer.
    In order to determine the temperature of the solid part of the turbine during transient behaviour can Euler forward be used as shown in Equation 3.6.

$$T_{t,sol}(i) = T_{t,sol}(i-1) + T_{step} \frac{T_{t,sol}(i-1)}{dt} \tag{3.6}$$

    $T_{t,sol}(i)$ is the turbine housing temperature in the current time step. $T_{t,sol}(i-1)$ is the turbine housing temperature in the previous time step, T_{step} the length of the time step made and $\frac{T_{t,sol}(i-1)}{dt}$ is the derivative of the turbine housing temperature in the previous time step.

3.3   Temperature change over exhaust manifold

There is a possibility that the exhaust gas temperature change over the exhaust manifold. Since the turbine inlet temperature affect the turbine outlet temperature, models concerning heat transfer in the exhaust manifold were investigated. The first model is presented in this section and the second model can be found in Appendix B since it was not implemented.
    The mass flow to the small turbine was ignored and the wastegate was closed. The temperature of the exhaust manifold walls were assumed to be uniformly distributed. The first model was built on a similar analysis as the one explained in section 3.2 but applied on the exhaust manifold. Even here the system could be simplified to one control volume for the gas and one of the solid part of the exhaust system. The energy flows considered for the gas control volume was the enthalpy change in the pipe and the convective heat transfer to the pipe. By integrating over the length of the pipe the exhaust manifold outlet temperature can be described by Equation 3.7. A detailed description of the steps is done in Eriksson [13].

$$T_{t,in} = T_w + (T_{m,in} - T_w)e^{-\frac{h_{w,in}A_w}{\dot{m}_{exh}c_{p,exh}}} \tag{3.7}$$

T_w is the mean wall temperature, $T_{m,in}$ and $T_{t,in}$ are the temperatures of the gas going to and from the exhaust manifold, $\dot{m}_{exh}$ is the exhaust gas mass flow and $c_{p,exh}$ is the specific heat capacity of the exhaust gas. The heat transfer coefficient $h_{w,in}$ was estimated from curve fitting under stationary load points and the inner area of the exhaust manifold, A_w, was estimated from CAD-models.

The energy flows considered for the solid part of the exhaust manifold are the convective heat transfer from the gases to the pipes and the convective and radiative heat transfer to the surroundings from the exhaust manifold surface. Conductive heat transfer from the engine to the two turbines were in a first try be modelled as constant due to the lack of measurements on the engine as well as on the small turbocharger. A controller was used to control the small wastegate to keep the small turbine in a low speed. If the turbine stops it might cause the oil through the bearing housing to stop flowing which could break the bearing housing. However, the mass flow through the small turbine was ignored during simulation. Application of the first law of thermodynamics for the solid control volume representing the exhaust manifold gives Equation 3.8.

$$\begin{aligned} m_w c_{p,w} \frac{dT_w}{dt} =\, & h_{w,in}A_w(T_{m,in} - T_w) - h_{w,out}A_w(T_w - T_{amb}) \\ & - \epsilon_w \sigma A_w(T_w^4 - T_{amb}^4) + \dot{Q}_{cond} \end{aligned} \tag{3.8}$$

m_w is the exhaust manifold mass and $c_{p,w}$ is the specific heat capacity of the exhaust manifold. $h_{w,in}$ and $h_{w,out}$ are the inside and outside heat transfer coefficients of the exhaust manifold. A_w is the area where heat transfer occur. $T_{m,in}$ is the exhaust gas temperature at the exhaust manifold inlet, T_w the exhaust manifold wall temperature and T_{amb} the ambient temperature. ϵ_w is the emissivity of the exhaust manifold wall and σ the Stefan-Boltzmann constant.

The first term on the right side of the equal sign represents convection from the gas to the wall. This expression is simplified to only use the inlet temperature as gas temperature. The second term is the convective heat transfer to the surroundings and thereafter is the radiative heat transfer to the surroundings. $\dot{Q}_{cond}$ is a constant representing all conductive heat transfer to and from the exhaust manifold. By doing tests under stationary load points could the left side of the equation be set to zero and the constants $h_{w,out}$, ϵ_w and $\dot{Q}_{cond}$ be determined.

By combining Equation 3.7 and 3.8 could the turbine outlet temperature be determined from exhaust manifold inlet temperature.

In order to determine the temperature of the exhaust manifold wall during transient condition was Euler forward used as shown in Equation 3.9.

$$T_w(i) = T_w(i-1) + T_{step}\frac{T_w(i-1)}{dt} \tag{3.9}$$

$T_w(i)$ and $T_w(i-1)$ are the wall temperatures in the current and last time step, T_{step} the time step length and $\frac{T_w(i-1)}{dt}$ is the derivative of the wall temperature.

4

Measurements

4.1 Measurements

This section contains information about how measurements were conducted and how the data was processed. The measurements were used to identify unknown parameters in the models described in chapter 3 and to validate the models.

4.1.1 Test setup

Measurements were conducted in an engine test rig at Linköping University in cooperation with Volvo Cars. The turbocharger used during measurements was a cast iron double turbo connected to an SI-engine. Engine load and speed was varied to achieve different exhaust mass flows and temperatures. The wastegate was kept closed during all measurements to ensure that all exhaust gases were forced to go through the turbine. A fan was faced towards the turbocharger to avoid overheating. For a vehicle in motion is the air surrounding the turbocharger flowing which gives corresponding effect as the fan.

4.1.2 Placement of sensors

Different sensors were used in the system to measure mass flows, fluid temperatures, housing temperatures and pressures. All the measurements that were conducted and used are presented in table 4.1.

The temperature measurements of the turbine housing were made with sensors attached to the surface, distributed over the exhaust manifold and the turbocharger. These sensors were used to get a better understanding of the temperature distribution and the mean temperatures were used to determine the convection and radiation. The placings of the surface thermocouples are shown in Figure 4.1. The thermocouples were glued to the surface as shown in Figure 4.3.

The placings of the gas temperature sensors and the pressure sensors are shown in Figure 4.2. The ambient pressure and temperature were used as the compressor intake temperature and pressure, and the temperature and pressure at compressor outlet were measured between the compressor outlet and the intercooler. The turbine inlet temperature and pressure were measured where the outlet from the small turbocharger and the exhaust manifold merge. The turbine outlet pressure was measured just after the expansion and the turbine outlet temperature was the temperature measured in the first brick of the catalyst. The temperature of the exhaust gas from the cylinders were measured next to two different exhaust ports.

Table 4.1: Measurements for heat transfer modelling

Measurement	Value	Description
Mass flow	$\dot{m}_{air}$	Mass flow of intake air $[kgs^{-1}]$
Fluid temperature	$T_{c,in}$	Air at compressor intake [K]
	$T_{c,out}$	Air at compressor outlet [K]
	$T_{m,in1}$	Exhaust gas from cylinders [K]
	$T_{m,in2}$	Exhaust gas from cylinders [K]
	$T_{t,in}$	Exhaust gas at turbine intake [K]
	$T_{t,out}$	Exhaust gas at turbine outlet [K]
	T_{oil}	Oil temperature [K]
	T_{amb}	Surrounding temperature of turbine [K]
Housing temperature	$T_{t,sol1}$	Turbine housing [K]
	$T_{t,sol2}$	Turbine housing [K]
	$T_{t,sol3}$	Turbine housing [K]
	$T_{t,sol4}$	Turbine housing close to catalyst [K]
	T_{c-b}	On compressor close to bearing housing [K]
	T_{t-b}	On turbine close to bearing housing [K]
	T_{w1}	Exhaust manifold wall close to wastegate [K]
	T_{w2}	Exhaust manifold wall close to turbine inlet [K]
	T_{w3}	Exhaust manifold wall close to cylinders [K]
	T_{w4}	Exhaust manifold wall close to cylinders [K]
Pressure	p_{01}	Pressure at compressor intake [Pa]
	p_{02}	Pressure at compressor outlet [Pa]
	p_{03}	Pressure at turbine intake [Pa]
	p_{04}	Pressure at turbine outlet [Pa]
	p_{oil}	Oil pressure $[kgs^{-1}]$
Other	ω_{tc}	Turbo speed [rps]
	λ	Lambda
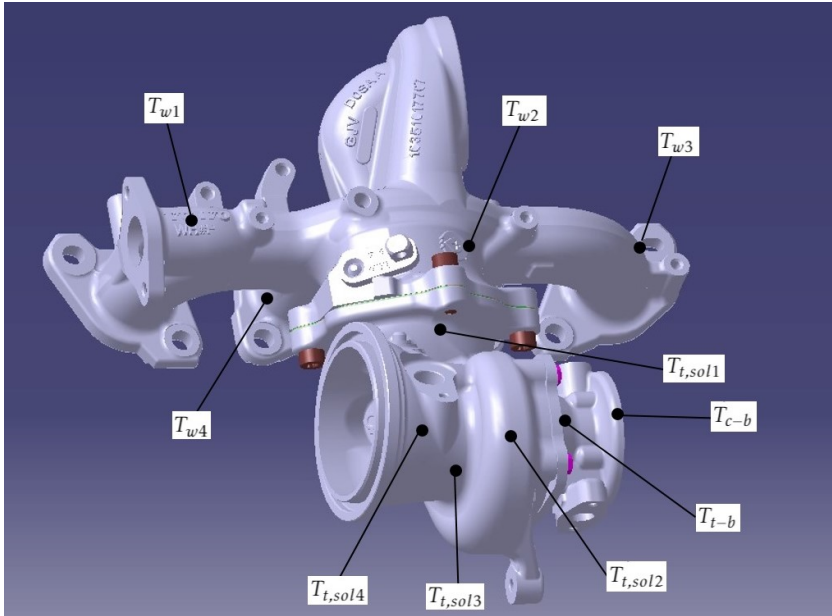
Figure 4.1: *Thermocouple placings on the exhaust manifold and the turbine housing.*
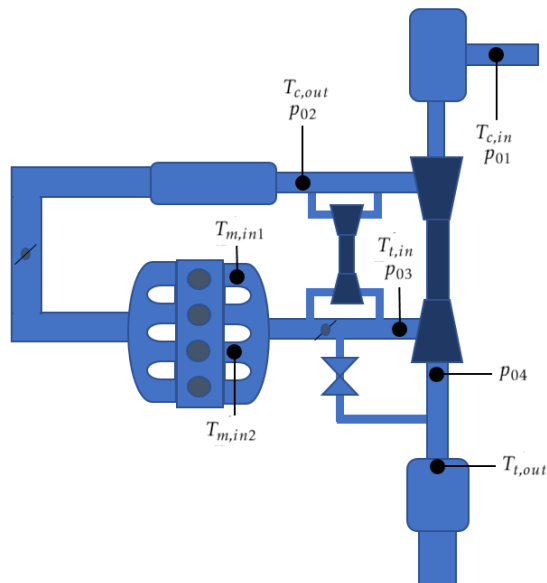
Figure 4.2: *Placing of sensors for measurements of gas temperatures and pressures.*

Figure 4.3: *Thermocouples glued on the turbine housing.*

The exhaust mass flow was calculated from the air mass flow, $\dot{m}_{air}$, air fuel ratio, AFs, and lambda value, λ as in Equation 4.1 and 4.2. $\dot{m}_{fuel}$ is the fuel mass flow.

$$\dot{m}_{fuel} = \frac{\dot{m}_{air}}{AF_s \lambda} \tag{4.1}$$

$$\dot{m}_{exh} = \dot{m}_{air} + \dot{m}_{fuel} \tag{4.2}$$

The oil mass flow and oil inlet and outlet temperatures from the turbine housing were wanted but not possible to access. Instead was oil pressure and total oil temperature measured. The oil mass flow and oil pressure are correlated which made it possible to estimate the oil mass flow according to Equation 4.3.

$$\dot{m}_{oil} = c\sqrt{p_{oil}} \tag{4.3}$$

$\dot{m}_{oil}$ is the oil mass flow, p_{oil} is the oil pressure and c is a constant which was estimated with least square method.

The mounting of the thermocouples was fragile and two sensors were damaged during transport and installation, one on the turbine next to the turbine housing, T_{t-b}, and one sensor on the exhaust manifold, $T_{w,4}$. The sensor marked T_{c-b} placed on the compressor close to the bearing housing was not responding. A temperature on the catalyst wall was wanted for estimation of conduction but was not possible to measure.

4.1.3   Constants

Material properties such as specific heat capacity and viscosity change with temperature. These changes were ignored since they are fairly small compared to the overall uncertainty of the models. The material properties have been taken at a mean value of the temperature and were obtained from [14], [3] and [12]. The viscosity of the exhaust gas was estimated as the viscosity of air. The turbocharger geometry values were estimated from a CAD model of the turbocharger. The material properties and geometries used are presented in Table 4.2.

Table 4.2: Constants necessary for heat transfer modelling

Type of parameter	Value	Description
Material properties	$c_{p,oil}$	Specific heat capacity oil $[Jkg^{-1}K^{-1}]$
	$c_{p,air}$	Specific heat capacity intake air $[Jkg^{-1}K^{-1}]$
	$c_{p,exh}$	Specific heat capacity exhaust gas $[Jkg^{-1}K^{-1}]$
	γ_{air}	specific heat ratio air
	γ_{exh}	specific heat ratio exhaust gas
	$(A/F)_s$	Air/Fuel ratio
Turbocharger geometry	$A_{w,in}$	Exhaust manifold inside area $[m^2]$
	$A_{w,out}$	Exhaust manifold outside area $[m^2]$
	V_w	Exhaust manifold volume $[m^3]$
	$A_{t,in}$	Inside area turbine $[m^2]$
	$A_{t,out}$	Turbine outside area $[m^2]$
	V_t	Turbine volume $[m^3]$
	d_t	Turbine diameter $[m]$

4.1.4   Engine load and speed

Measurements were conducted for stationary operating conditions with different engine loads and speeds. The loads were varied to achieve different turbine inlet temperatures, pressures and mass flows. The load points used are presented in Table 4.3.

The measurements were conducted under stationary conditions. For each load point equilibrium was reached after approximately 15 minutes. All signals were then sampled for approximately 10 seconds. The sampling frequency differed between different sensors. The mean value from each sample was used for the modelling.

Table 4.3: Stationary load points

Load Speed	15 Nm	20 Nm	35 Nm	55 Nm	95 Nm	110 Nm	135 Nm
1000 rpm		X		X	X	X	
1250 rpm	X		X	X	X		
1500 rpm		X		X	X		X
2000 rpm		X		X	X		X
2500 rpm		X		X	X		X
2750 rpm		X		X	X		X
3000 rpm		X		X	X		X
3500 rpm		X		X	X		

4.2   Impact of pulsating flow

The sensors used for measuring fluid temperatures measure the temperature of the gas flow. Since the sensor itself has a thermal mass is not able to follow fast temperature changes [31]. Such changes may occur due to pulsations in the flow which will be perceived as averaging. Since all measurements are conducted in an engine rig the flow will be pulsating due to the cycles of the cylinders. The effect of the pulsations will be more significant at the exhaust manifold inlet than at the exhaust manifold outlet. Since the exhaust manifold gathers the exhaust gases from the four cylinders the pulsations will be smaller and the mean temperature higher since they all work coordinated.

The design of turbochargers is most suitable for steady flow, while it is often exposed to unsteady flow when connected to a combustion engine [23]. The pulsations give mechanical losses in the turbocharger that is not constant even during stationary operation. It is important to consider the variations of turbine power output and mechanical losses while building models since non-linearities affect the result during 1 dimensional modelling.

4.3   Heat transfer in thermocouples

It is important to be aware of that the temperature sensors might be influenced of the environment and not always show the temperature that is expected.

The sensors used to measure the temperatures of the solids are placed on the outside only. They were isolated but it should be considered that convection to the environment might lead to that the sensors show a lower temperature than is measured on the surface. It is also important to remember that there is a temperature gradient within the material due to different temperatures on the outside and the inside.

The sensors used to measure the gas temperature has the uncertainties that it is fixed to the housing wall. The thermocouple might be effected by radiation and conduction from the housing, and not only by convection from the gas. when there is a temperature difference between the wall temperature and the gas there is a big risk of conduction along the thermocouple itself. Radiation from the walls to the thermocouple might affect the measured temperature to be higher than the gas temperature.

5

Implementation

5.1 Turbine outlet temperature

This section contains descriptions on how the implementation of the lumped capacitance model for the turbine was made. Some adjustments were made to get a better fit or to simplify the model. Due to time limitations the models were only implemented for stationary load and speed. The heat transfer coefficients where determined in two steps, first the coefficient affecting the heat transfer from the gas to the housing and thereafter the heat transfer from the solid to the surrounding together with the emissivity of the turbine. To compare the different options were the absolute and relative error used as described in equation 5.1 and 5.2.

$$Absolute\ error = T_{measured} - T_{model} \tag{5.1}$$

$$Relative\ error = \frac{T_{measured} - T_{model}}{T_{measured}} \times 100 \tag{5.2}$$

5.1.1 Turbine housing temperature

The measurements from the different sensors placed on the turbine housing are shown in Figure 5.1. There is a large temperature difference between the different sensors, up to 107 K for some load points. Since the sensors were affected in differing extent of radiation and forced convection it was difficult to determine the temperature distribution of the turbine and a mean value of the sensors gave the mean temperature of the turbine. As shown in Figure 5.1 there is a linear relationship between turbine housing temperature and turbine inlet temperature.
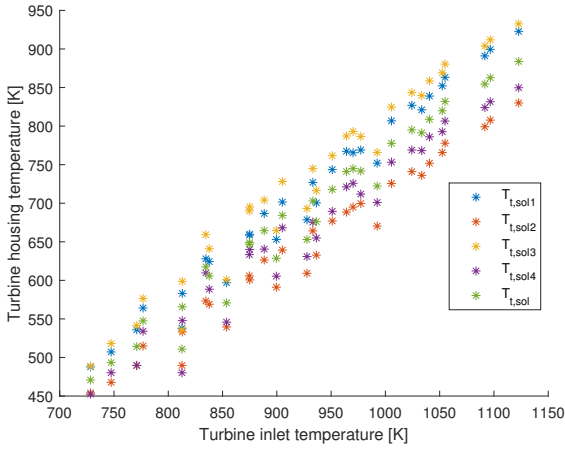
Figure 5.1: *Turbine housing temperatures*

5.1.2 Heat transfer coefficient inside

First the influence of the use of different gas temperatures for inside convection was investigated. The heat transfer coefficient was modelled as constant and the friction was neglected. The heat transfer coefficient on the inside was modelled as in Equation 3.2 with $T_g = T_{t,in}$, $T_g = T_{t,out}$ and $T_g = \frac{T_{t,in}+T_{t,out}}{2}$. Table 5.1 shows the relative and absolute error between the modelled and measured turbine outlet temperature. It is shown that the relative and absolute error is smallest when $T_g = T_{t,in}$ and for the following modelling will therefore the assumption that $T_g = T_{t,in}$ be used. Different weighting between inlet and outlet temperature was also tried out, however no result was better than for $T_g = T_{t,in}$.

Table 5.1: *Absolute and relative error for different options of T_g*

	Max absolute [K]	Mean absolute [K]	Max relative [%]	Mean relative [%]
$T_g = T_{t,in}$	32.4	10.1	5.5	1.3
$T_g = T_{t,out}$	48.6	11.1	8.3	1.4
$T_g = \frac{T_{t,in}+T_{t,out}}{2}$	40.4	10.6	6.9	1.3

In the first attempt of determining the inside heat transfer coefficient, $h_{t,in}$ it was modelled as constant. However, for forced convection is the heat transfer coefficient highly dependent on the velocity of the fluid as described in Section 2.3.2. Since the geometry and the conditions inside the turbocharger is difficult to determine, an attempt to model the heat transfer coefficient as a second order polynomial was tried out as shown in Equation 5.3, where h_0, h_1 and h_2 are constants found through least square method and $\dot{m}_{exh}$ is the exhaust mass flow.

$$h_{t,in} = h_0 + h_1 \dot{m}_{exh} + h_2 \dot{m}_{exh}^2 \tag{5.3}$$

When trying this out $h_{t,in}$ was decreasing with increasing exhaust mass flow, opposite what was expected. It was then tried to model it as a first order polynomial and as a second order polynomial where h_1 was set to zero. The result of both these cases were that the heat transfer coefficient was decreasing with increasing exhaust mass flow and this option was a bad alternative.

Another method was tried out with the intent to model the heat transfer coefficient from known correlations. The turbine was approximated as a pipe. For turbulent flow inside of smooth tubes can Equation 5.4 to 5.7 be used to determine the heat transfer coefficient.

$$Re = \frac{v_{avg} D}{\nu} \tag{5.4}$$

The Reynolds number Re can be determined from the average velocity of the fluid, the diameter of the pipe and the viscosity ν of the fluid.

$$Pr = \frac{\mu c_p}{k} \tag{5.5}$$

The Prandtl number is determined from the thermal conductivity k, the specific heat capacity c_p and the dynamic viscosity μ. The Nusselt number can then be described from Equation 5.6.

$$Nu = 0.023 Re^{0.8} Pr^{1/3} \tag{5.6}$$

That gives the heat transfer coefficient according to Equation 5.7.

$$h = \frac{k Nu}{L} \tag{5.7}$$

Since everything besides the velocity from these equations are constants the heat transfer coefficient was estimated from Equation 5.8

$$h_{t,in} = c \dot{m}_{exh}^{0.8} \tag{5.8}$$

Where c is a constant approximated with least square method. That gave a modelled value of the turbine outlet temperature with a maximum relative error of 15.0% and a mean relative error of 2.2% when compared to measurements from sensor $T_{t,out}$. Since the model with a heat transfer coefficient determined as in Equation 5.8 performed worse compared to the model with constant $h_{t,in}$, the heat transfer coefficient was therefore modelled as a constant.

Further attempts to improve the result was done by introducing a term describing the friction power in the bearing housing. This was introduced as in Equation 5.9 where the friction power was assumed to increase linearly with the turbine rotational speed, ω_{tc}.

$$W_{fric} = a_1 + a_2 \omega_{tc} \tag{5.9}$$

a_1 and a_2 are constants. However, these constants were negative, opposite what was expected [11] and the losses due to friction was further ignored.

The model validation for the heat transfer coefficient on the inside is shown in Figure 5.2. The turbine outlet temperature estimated using Equation 5.11 show an acceptable agreement with measured data on the measured temperature from sensor $T_{t,out}$. However, the fit between modeled and measured values of the turbine outlet temperature is worse for low turbine inlet temperatures.
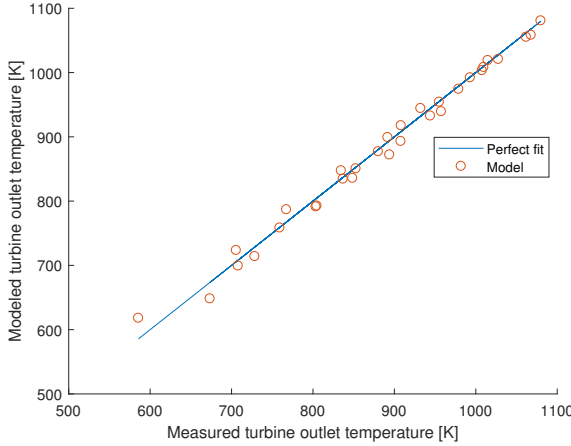
Figure 5.2: *Model validation, heat transfer coefficient inside*

The relative error between measured and modeled values on the turbine outlet temperatures with respect to mass flow and turbine inlet temperatures is shown in Figure 5.3. The magnitude of the error is greater for low mass flows and low inlet temperatures.

The heat transfer coefficient for the inside was determined to $h_{t,in} = 43.6$ from the final model in Equation 5.10.

$$\dot{m}_{exh}c_{p,exh}(T_{t,in} - T_{t,out}) = h_{t,in}A_{t,in}(T_{t,in} - T_{t,sol}) + \dot{m}_{air}c_{p,air}(T_{c,out} - T_{c,in}) \quad (5.10)$$

By rewriting Equation 5.10 the turbine outlet temperature can be described as a function of the exhaust mass flow, air mass flow, turbine inlet temperature, compressor inlet temperature and compressor outlet temperature. This is described in Equation 5.11.

$$
\begin{aligned}
T_{t,out} &= f\left(\dot{m}_{exh}, \dot{m}_{air}, T_{t,in}, T_{c,in}, T_{c,out}, T_{t,sol}\right) \\
&= T_{t,in} - \frac{h_{t,in}A_{t,in}(T_{t,in} - T_{t,sol}) + \dot{m}_{air}c_{p,air}(T_{c,out} - T_{c,in})}{\dot{m}_{exh}c_{p,exh}}
\end{aligned} \quad (5.11)
$$
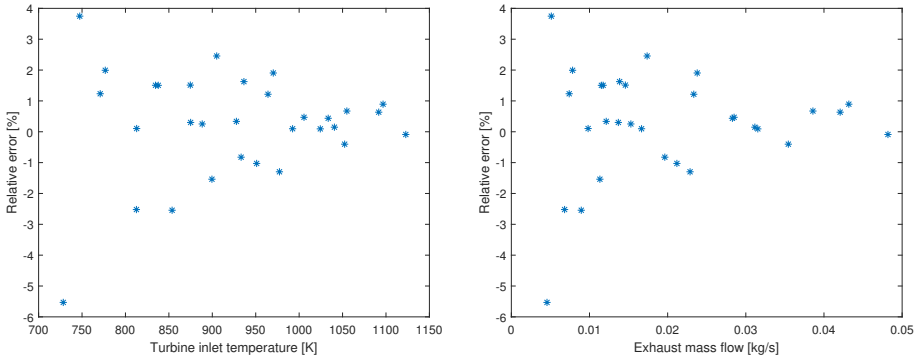
Figure 5.3: *Relative error of the model concerning heat transfer on inside of the turbine. The left plot shows the relative error with respect to turbine inlet temperature and the right plot shows the relative error with respect to exhaust mass flow*

5.1.3   Heat transfer coefficient outside

The model used to determine the heat transfer coefficient on the outside was first described in Equation 3.4. However, it was not possible to measure the oil temperature just before and after the bearing housing and it was therefore not used. It was neither possible to determine the conduction through the material through measurements and those terms were ignored.

The model used in this first iteration is described in Equation 5.12. The heat transfer coefficient on the inside, $h_{t,in}$, was the one determined in the previous step. To get reasonable values on $h_{t,out}$ and ϵ_t they were limited as described below.

$$h_{t,in} A_{t,in} (T_{t,in} - T_{t,sol}) = h_{t,out} A_{t,out} (T_{t,sol} - T_{amb}) + \epsilon_t \sigma A_{t,out} (T_{t,sol}^4 - T_{amb}^4) \quad (5.12)$$

$$25 \leq h_{t,out} \leq 250$$

$$0 \leq \epsilon_t \leq 1$$

The validation of this model is shown in Figure 5.4 where the turbine inlet temperature estimated from Equation 5.12 is compared to measured values from sensor $T_{t,in}$. There are big errors between measured and modeled turbine inlet temperature with a maximum absolute error of 178.9 K and a maximum relative error of 22.0 %. This estimation gave parameter values on or close to the lower limit, $h_{t,out} = 25$ and $\epsilon_t = 2.3 \cdot 10^{-14}$. One possible reason for the big error is that the conduction heat transfer was not included.
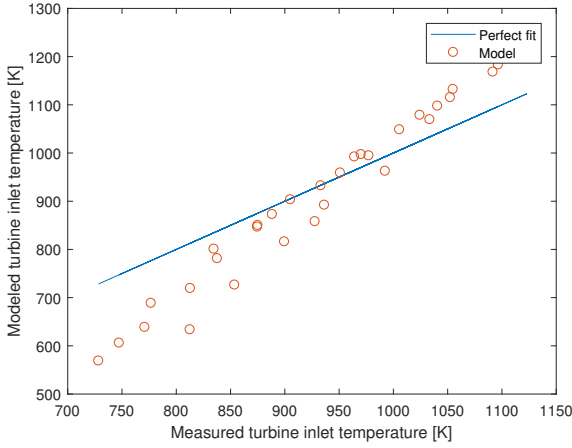
Figure 5.4: *Model validation, heat transfer coefficient outside*

An attempt to include the conductive heat transfer was made by introducing a first order polynomial as described in Equation 5.13. It is dependent on the turbine housing temperature since that is the only conductive surface with known temperature. The new model with conduction included is described in Equation 5.14.

$$\dot{Q}_{cond} = c_1 + c_2 T_{t,sol} \tag{5.13}$$

$$
\begin{aligned}
0 =& h_{t,in} A_{t,in} (T_{t,in} - T_{t,sol}) - h_{t,out} A_{t,out} (T_{t,sol} - T_{amb}) \\
&- \epsilon_t \sigma A_{t,out} (T_{t,sol}^4 - T_{amb}^4) - \dot{Q}_{cond}
\end{aligned}
\tag{5.14}
$$

The turbine inlet temperature estimated with Equation 5.14 was compared with the measured value on the turbine inlet temperature from sensor $T_{t,in}$. As shown in Figure 5.5 the fit was improved when an additional term for conduction was added. The heat transfer coefficient and the emissivity showed more reasonable values for this model, $h_{t,out} = 54.37$ and $\epsilon_t = 0.103$. The constants for the conduction was $c_1 = 2266.4$ and $c_2 = -4.51$.
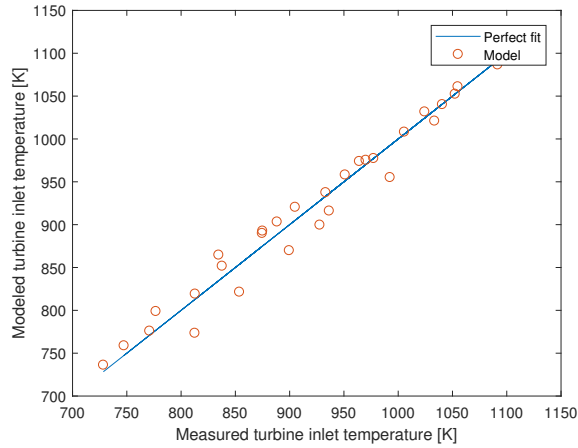
Figure 5.5: Model validation, heat transfer coefficient outside

The relative error between the turbine inlet temperatures modeled with Equation 5.14 and the measured value on the turbine inlet temperature was plotted with respect to mass flow and turbine inlet temperature. This is shown in Figure 5.6. Even here is it clear that the magnitude of the error is greater for low turbine inlet temperatures and for small exhaust mass flows.
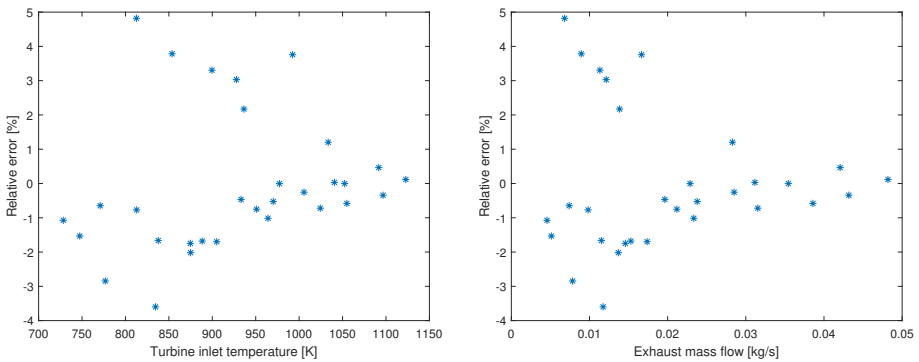
Figure 5.6: Relative error of the model concerning heat transfer on outside of the turbine. The left plot shows the relative error with respect to turbine inlet temperature and the right plot shows the relative error with respect to exhaust mass flow.

An attempt to simplify the model by using the linearized version of the radiation equation was made. This led to an outside heat transfer coefficient that included both convection and radiation. Equation 5.15 describes the linearized version of the model. A comparison between the modeled value on the turbine inlet temperature using the model from Equation 5.15 and measured value from

the sensor $T_{t,in}$ is shown in Figure 5.7.

$$0 = h_{t,in} A_{t,in} (T_{t,in} - T_{t,sol}) - h_{t,out} A_{t,out} (T_{t,sol} - T_{amb}) - \dot{Q}_{cond} \qquad (5.15)$$
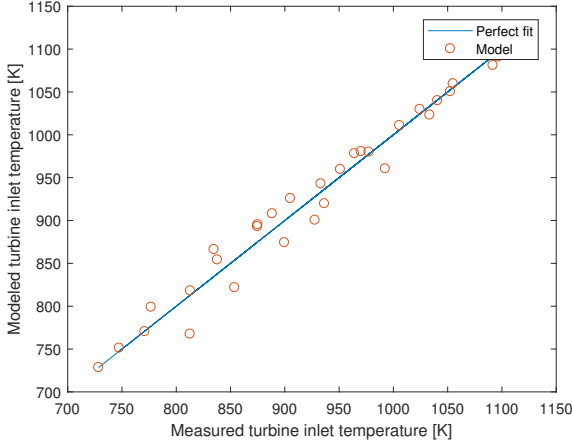
Figure 5.7: Model validation, heat transfer coefficient outside, linearized version

Values on the estimated errors from the models described in Equation 5.14 and 5.15 are shown in table 5.2. The error was bigger for the linearized version, as expected. The final model concerning external heat transfer during stationary condition is described in Equation 5.16.

Table 5.2: Absolute and relative error for modelled values on $T_{t,in}$ with and without a separate parameter for radiation

	Max absolute [K]	Mean absolute [K]	Max relative [%]	Mean relative [%]
Normal	39.2	13.3	4.8	1.5
Linearized	45.0	14.2	5.5	1.6

$$\begin{aligned} 0 = & h_{t,in} A_{t,in} (T_{t,in} - T_{t,sol}) - h_{t,out} A_{t,out} (T_{t,sol} - T_{amb}) \\ & - \epsilon_t \sigma A_{t,out} (T_{t,sol}^4 - T_{amb}^4) - c_1 - c_2 T_{t,sol} \end{aligned} \qquad (5.16)$$

By rewriting Equation 5.16 can the turbine inlet temperature be described as a function of turbine housing temperature and ambient temperature as described in Equation 5.17.

$$T_{t,in} = f\left(T_{t,sol}, T_{amb}\right) =$$

$$T_{t,sol} + \frac{h_{t,out}A_{t,out}(T_{t,sol} - T_{amb}) + \epsilon_t\sigma A_{t,out}(T_{t,sol}^4 - T_{amb}^4) + c_1 + c_2 T_{t,sol}}{h_{t,in}A_{t,in}} \quad (5.17)$$

The Biot number, Bi, was controlled by using the highest calculated value on the heat transfer coefficient, $h = 54.4$, together with the thermal conductivity for cast iron, $k = 52W/mK$ [29] and the volume and area of the turbine. Giving the Biot number according to Equation 5.18. The calculated Biot number is well below lowest allowed value of $Bi < 0.1$.

$$Bi = \frac{hV}{kA} = 0.015 \quad (5.18)$$

5.2   Temperature change over exhaust manifold

The exhaust gas temperatures were measured at three different places in the exhaust manifold. There were sensors placed next to two of the exhaust ports and one at the turbine inlet. These temperatures can be seen in Figure 5.8. There was a big difference between the exhaust temperatures from the exhaust ports, up to 72.5 K. For exhaust manifold inlet temperature was a mean temperature from the temperatures from exhaust port 1 and 2 used. There is an increase of the exhaust gas temperature over the exhaust manifold.

Also the exhaust manifold wall temperatures are shown in Figure 5.8. Here the difference between the different sensors was as much as 222.2 K in some load points and the mean difference between the first and second sensor, T_{w1} and T_{w2}, was in 185.1 K.
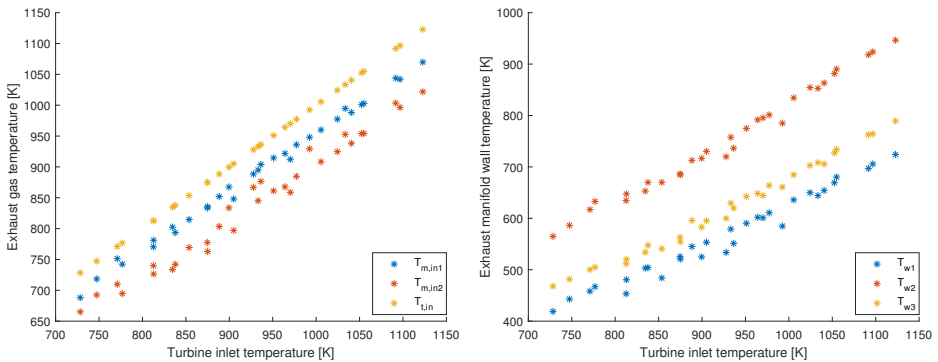
Figure 5.8: *Temperatures on exhaust gas in the exhaust manifold is shown in the plot to the left and wall temperatures on the exhaust manifold housing is shown to the right*

The lumped capacities model for the exhaust manifold described in section 3.3 was not implemented since the temperatures did not act as expected.

Both exhaust manifold inlet and exhaust manifold outlet temperatures are higher than the average wall temperature. However, this would mean that there would be heat transfer from the gas to the wall, as expected. However, this should mean that there should be a temperature drop of the gas over the exhaust manifold, which is not the case. Instead the gas temperature increase over the exhaust manifold. The most probable reason for this should be that heat is transferred from the walls to the exhaust gas, however, measurements show that all wall temperatures are lower than both inlet and outlet temperatures of exhaust gas. The measurements of exhaust manifold wall is made on the outside and may be affected by convective heat transfer. There is also a temperature gradient in the material which might lead to a lower measured value than there is on the inside of the exhaust manifold. Since the measurements are not enough to make any reasonable conclusions was the implementation of the exhaust manifold models assumed not to be valid.

6

Result

6.1 Turbine outlet temperature

To get a better understanding of which heat flows that occur around the turbine, the modelling was divided into two steps. First the heat transfer from the exhaust gas to the turbine housing was determined. The turbine outlet temperature can be described as a function of the exhaust mass flow, air mass flow, turbine inlet temperature, compressor inlet temperature and compressor outlet temperature as in Equation 5.11. The result from this model is shown in Figure 6.1 where modelled and measured values on the turbine outlet temperature is plotted against the engine speed and engine load. The convective heat transfer coefficient was modelled as constant and the friction losses in the bearing housing ignored. The modelled values show good agreement for the majority of the chosen load points. However, the model has less accuracy for low engine torques and low engine speeds. However, it shows a fairly good fit.

The result from the modelled heat transfer concerning the solid part of the turbine is shown in Figure 6.2 where the modelled and measured values on the turbine inlet temperature is plotted against the engine load and speed. The turbine inlet temperature can be described as a function of the turbine housing temperature and the ambient temperature as described in Equation 5.17. The model includes the convective heat transfer where the convective heat transfer coefficient is modelled as constant, the radiation where the temperature of the surrounding objects is estimated to surrounding temperature and the conduction is modelled as a linear function depending on turbine housing temperature. Since the inside heat transfer coefficient is used here as well it might lead to slight inaccuracies. It is clear however that the model has pretty good overall agreements, but it performs worse for low engine loads.
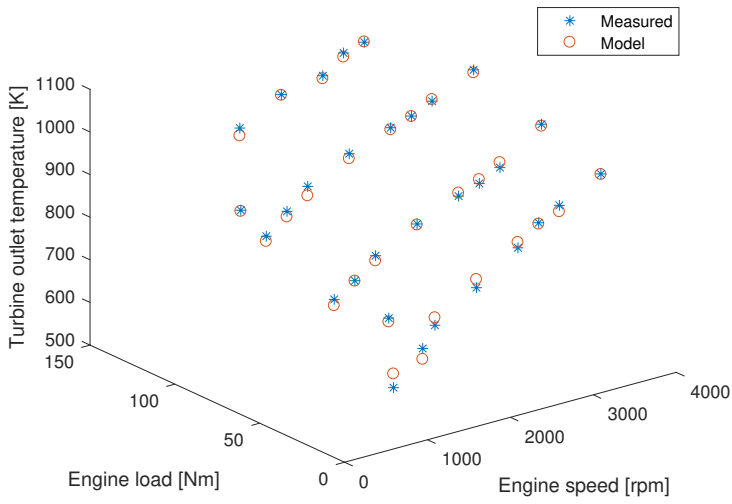
Figure 6.1: *Result of the model concerning heat transfer from exhaust gas to turbine housing*
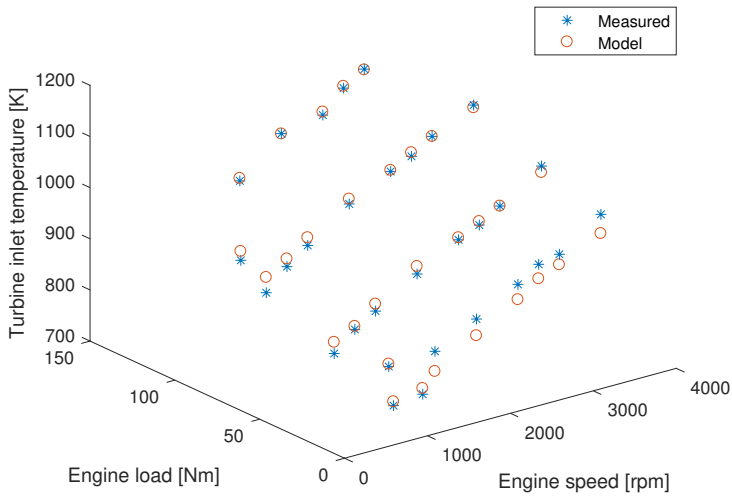
Figure 6.2: *Result of the model concerning heat transfer from the turbine housing to its surroundings*

The obtained design parameters are presented in Table 6.1. The heat transfer coefficients are within the limits of what is expected for forced convection. The heat transfer coefficient on the inside is slightly lower than expected due to the velocities in the turbine. The extra parameters for conduction indicate that heat is transferred through conduction from the turbine at low speeds and to the turbine at high speeds.

Table 6.1: Obtained values on design parameters

Parameter	Value	Unit
$h_{t,in}$	43.6	$[W/m^2 K]$
$h_{t,out}$	54.4	$[W/m^2 K]$
ϵ_t	0.103	$[-]$
c_1	2266.4	$[W]$
c_2	-4.51	$[W/K]$

The final models described in Equation 5.11 and 5.17 perform with a mean error of 1.3% and 1.5% respectively while their maximum error is 5.5% and 4.8% respectively.

The estimated energy flows are shown in Figure 6.3 and 6.4. The energy flows for the gas control volume is the enthalpy change in the gases, the convective heat transfer to the turbine housing and the work transfer through the turbocharger shaft. As shown in the figures the estimated heat transfer due to convection decrease with increased mass flow and turbine inlet temperature while the work transfer increase. This model does not consider the friction power used by the bearing housing.

The energy flows connected to the turbine housing is the convective heat transfer from the gas, the convective heat transfer to the surrounding, the radiation to the surroundings and the conduction through the material. As shown in Figure 6.4 the heat flow due conduction is changing its direction depending on working point. For low mass flows and exhaust temperatures is the heat flow through conduction going from the turbine housing to the connecting parts.

6.2   Exhaust manifold temperatures

The measurements of the exhaust manifold wall and gas temperatures showed to be not accurate to model on and no result was therefore obtained for this part. Even though it probably is possible to model the exhaust temperatures these would not have any physical connection.
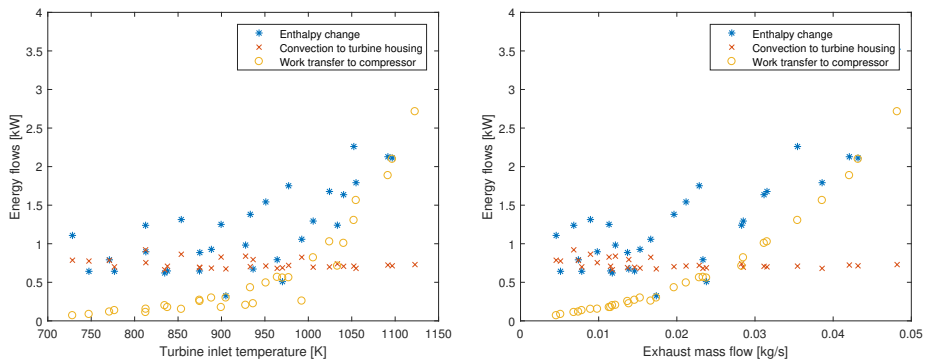
Figure 6.3: Energy flows concerning the gas control volume
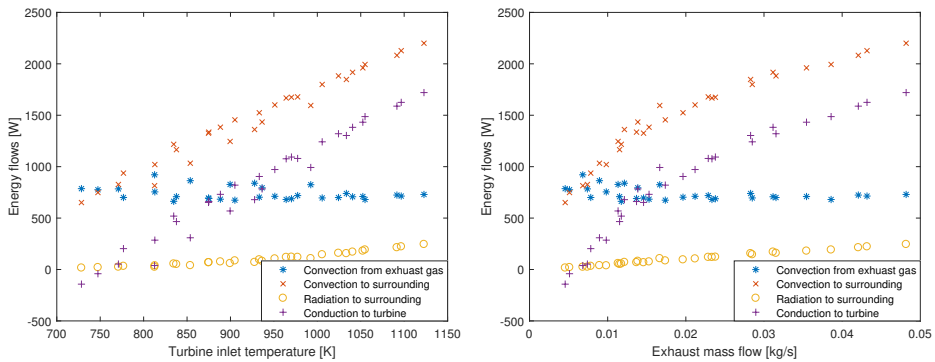
Figure 6.4: Energy flows concerning the solid control volume

6.3 Analysis of the result

As stated in section 2.4 is the effect of the heat transfer of the compressor more prominent for low mass flows and low rotational speeds. This could explain why the error is bigger for lower temperatures and mass flows since the heat transfer in the compressor is not included. This might also be part of the error even at higher loads and speeds, although less prominent.

There are several studies that show the radiation and convective heat flows affecting the performance of the turbocharger most. This is not what is shown through the results from this project. This shows that the conduction is of bigger importance than the radiation. A reason for this could be that the convection from the turbine to the surroundings is overestimated or that the convection from the gas to the housing is underestimated.

7

Discussion

7.1 Discussion

This section contains discussions about the design choices made and the obtained results. The discussion also covers possible improvements in the approach of the problem.

7.1.1 Modelling

The turbocharger used during modelling was a double stage turbocharger, but it was modelled as a single stage turbocharger. The small turbocharger was not considered at all but could probably be included in the future. The effects of the wastegate was also ignored by only making measurements in load points where a closed wastegate is possible. Despite that the model developed for the big turbocharger is promising, even though it might need some improvement.

Mean value modelling was chosen for two reasons. The first is that it is what is used for the control oriented engine models, making it easier to integrate it into the full engine simulation code. The second is that the sensors used do not manage to measure the influence of the pulsations with enough accuracy.

Two different models were used for modelling of the heat transfer effect on the turbocharger. The reasons for this was to increase the chances of finding a model performing as good as possible with fairly simple measurements. The first model used, the lumped capacitance model, was used to get a better understanding of the heat flows concerning the turbocharger. The second model was chosen for its simplicity, however no results were obtained for the second model. An attempt to find a heat transfer model for the exhaust manifold was made since the temperature change over the exhaust manifold has an impact in the turbine inlet temperature.

During the modelling several assumptions and simplifications were made. As far as possible these simplifications were evaluated or enhanced by measurements. The convection from the gas to the turbine housing was assumed to occur with a constant gas temperature, even though its temperature is changing through the turbocharger. This was because it is difficult to investigate exactly how the temperature changes over the turbine. The work transferred through the shaft was calculated from the work used by the compressor. As stated in the related research the heat transfer is also affecting the compressor. By including the heat transfer effects on the compressor side as well a better result could probably be obtained. However, since the focus of this thesis was on the turbine and the heat transfer to the compressor was assumed to give a smaller influence, the heat transfer of the compressor was ignored. To include the conduction as intended initially heat transfer rates would be needed, values that are not normally obtained during simulation. An alternative way of modelling the conduction could therefore have been presented already during the modelling stage, instead of dealing with that problem during implementation. The heat transfer coefficient on the inside is probably changing both over time and through the turbocharger. Due to the complicated geometry of the turbocharger was no attempt to determine the Reynolds or Nusselt number made. This could otherwise be a way to get a better estimation of the heat transfer coefficient.

The second model for the turbocharger was simpler to implement, however due to lack of measurements no valid result was obtained. One way to model this could have been to try to find other correlations between parameters normally obtained during simulation. However, that would not increase the understanding of how different heat flows affect the turbocharger.

During modelling the exhaust manifold was assumed to consist of one single straight pipe which is far from its actual geometry. However, this was just an initial estimation and it could have been changed if it turned out to be a problem. In the first model, the conduction to other parts is very simplified and in the second model entirely neglected. Due to the big temperature differences the conduction have a fairly big impact on the result. For the first model the convection assumed to happen with a constant gas temperature through the pipe. Measurements showed it difficult to use any of the models for heat transfer in the exhaust manifold and no improvements were therefore not suggested. The reason for this was that the gas temperature increased over the exhaust manifold, indicating that heat is transferred from the exhaust manifold walls to the gas. However the wall temperatures were lower than the gas temperatures. One reason for this could be that the sensors are cooled by convection and the temperature perceived on the outside cannot be assumed to be equal to the temperature on the inside of the pipe.

7.1.2   Measurements

The errors from the measurements will cause inaccurate parameterization of the models and it is important to be aware of the errors and prevent as much of it as possible. To improve the result are some ways to improve the measurements

provided in this section. Measurements were only done on one turbocharger in one specific test rig. This affects the generality of the result. It is also important to be aware of that different conditions are applied for an engine with turbocharger on a vehicle.

To get a better knowledge of the heat transfer to and from the compressor it would be preferable to have more housing temperatures of the compressor housing as well as the bearing housing. By placing thermocouples on the small turbocharger would the possibilities to include the small size turbocharger in the models increase. To get a better estimation of the temperature of the turbine housing and the temperature gradient from inside to outside could sensors be placed in the goods. The temperature measurements of the turbine could have been done more extensively to get a better understanding of the temperature distribution over the turbocharger. Since the thermocouples are placed on the surface they are exposed to convective heat transfer in varying extent which affect the result. In order to get a better estimation of the temperatures an infrared camera could be used to determine the surface temperatures. One difficulty with this is that part of the turbocharger could be difficult to access with a camera.

There was a large temperature difference between the two temperature sensors in the exhaust manifold. To use only three surface thermocouples was not enough to measure the temperature of the exhaust manifold. It could also be seen in the temperature differences between sensors placed in the gas flow on corresponding places. One reason for the differences of the gas temperatures is that the temperatures may differ between the cylinders. It is also possible that the gas sensors are placed on different depth in the exhaust pipe. This would make a difference in how much the perceived gas temperature was influenced by conduction from the exhaust pipe. The fact that the temperature of the gas increased even though the surface temperatures were lower than the gas temperatures indicates that the temperature gradient within the turbocharger is not neglectable.

The measurements of the fluid temperatures are probably influenced by pulsations. This could be avoided by making tests in a constant flow test rig and not having the turbocharger attached to an engine. However, then it would be even more difficult model the conductive heat transfer to or from the parts connected to the turbine. Another cause of error is that the sensors measuring gas temperatures are exposed to heat transfer as well. For example, through radiation from the walls or through conduction along the sensor from the wall. The convection will probably also affect the measurements from the fluid sensors.

The oil mass flow was not possible to measure and instead estimated from oil pressure. In the end, this was not possible to use since the inlet and outlet oil temperature was not possible to measure. Constants were taken from look up tables at a mean value from measurements. This could have been improved by having a vector with different values on constants depending on temperature. This is on the other hand not estimated to have that big of an influence on the final result.

One way to isolate different heat transfer effects could be to try to isolate the turbocharger. For example, with radiation shields between the turbine and the compressor or with insulation material to avoid convection and radiation to the

surrounding. By comparing the result from the insulated measurements could maybe a better understanding of the effect concerning heat transfer on the turbocharger be achieved. Another problem that occurred was that the thermocouples were fragile and loosened easily. Another way to attach the sensors could be useful, maybe through welding. The insulation on the wires made them less flexible and probably more fragile against movement.

7.1.3   Implementation

Different options to implement the models were evaluated to achieve models estimating turbine outlet temperature with sufficient accuracy and with reasonable heat transfer coefficients. The implementation of the model concerning heat transfer from the gas to the turbine housing showed good result for high temperatures and mass flows, however the error was increasing with decreasing temperatures and exhaust mass flows. Something that probably is of importance is the heat transfer to the compressor and the friction losses in the bearing housing. A simple model to account for the friction losses was tried out, but with unsatisfying results. More research on this should be made so that it can be included in the model. One way to model the friction losses is to assume that they are corresponding to the enthalpy drop in the oil over the bearing housing. A problem with this is that the oil also acts a coolant and the temperature gain in the oil is both due to friction and from heat transfer from the turbine.

More effort should also be put in finding a model with a heat transfer coefficient that is changing with exhaust mass flow.

The model described with Equation 5.16 has the disadvantage of having to use the heat transfer coefficient from gas to turbine housing estimated in previous step. That could explain why the errors for low engine loads and speeds are higher than for higher engine loads and speeds. The first estimation showed fairly bad fit and was therefore extended with parameters that could correspond to the heat transfer caused by conduction. These would need further investigation under other heat transfer conditions to show their validity, however the result is promising.

The estimated Biot number was well within the acceptable margins. Even though there are some errors concerning the estimation of volume and area is the calculated Biot number well below the lowest allowed value, and the approach of lumped capacities should be valid.

7.1.4   Result

The result showed that the model performs worse for low temperatures and low exhaust mass flows which was expected. It could be caused by the heat transfer affecting the calculated work of the compressor. Heat transfer has a bigger impact at low engine speeds and loads.

The errors from the calculations of the inside heat transfer coefficient leads to more errors when estimating the external heat flows. The convective heat transfer to the surrounding and the radiation was believed to have the biggest impact,

however the radiation showed a fairly small impact on the overall heat transfer. One reason for this could be that the convective heat transfer gets an overestimated value. The conduction to other connecting parts does probably have an influence, however the estimated value of the conduction is higher than expected. Since the temperatures of the surrounding objects was unknown was the ambient temperature used when calculating the radiation, which could be a reason for the low estimated value on the emissivity.

8

Conclusion

8.1 Conclusion

A model for the heat transfer in the turbocharger was successfully implemented and evaluated. The result is a model with good agreement for high engine loads and speeds but which needs some improvement for lower engine speeds and loads. The model describes the heat transfer between the turbine and its surroundings and the magnitudes of different heat flows is estimated.

The model chosen for the turbine heat transfer shows reasonable result but would probably need some improvement. Improvements that could be made is to include the friction work in the bearing housing and the heat transfer to the compressor in the model.

8.2 Future work

There are several improvements that can be made to the model to make it reflect reality better. Especially the model concerning heat transfer in from the gas to the turbine housing needs further investigation. Improvements that are believed to make a difference on the final result is to include the friction in the bearing housing and to find a heat transfer coefficient that changes with exhaust mass flow. The heat transfer to the compressor is also believed to have a considerable effect and should be included in the model.

By insulating the turbocharger in different ways with for example radiation shields and insulation can convection and radiation to the surroundings be minimized. By comparing the measurements from the turbine with and without insulation could the external heat transfer through radiation and convection be evaluated. To get a better perception of the temperature distribution over the turbocharger and exhaust manifold a larger number of thermocouples or an infrared

camera could be used.

As future work should also the small turbocharger be included. It should also be investigated how the mass flow through the wastegate affects the heat transfer.

The model should also be tested and evaluated under transient conditions. That could be made by performing a step in throttle angle for example. Once the heat transfer effects are well known they should be implemented in an engine simulation to get an estimate of how much improvement the inclusion of heat transfer effect would generate on fuel consumption, emissions and driving experience.

A

Turbine outlet temperature, Method 2

The work made in this section is inspired by the work made by Ahgali and Ångström in [1]. The temperature of the bearing housing, T_{bh} can be found from Equation A.1 and the temperature of the turbine housing, $T_{t,sol}$, can be found from Equation A.2. Thereafter can the turbine outlet temperature be determined from Equation A.3.

$$\frac{T_{t,in} - T_{bh}}{T_{c,in}} = a_1 \left(0.9 \frac{T_{t,in} - T_{oil,in}}{T_{c,in}} + 0.1 \frac{vel}{vel_{max}} \right) + b_1 \tag{A.1}$$

$$\frac{T_{t,in} - T_{t,sol}}{T_{c,in}} = a_2 \left(\frac{T_{t,in} - T_{bh}}{T_{c,in}} \right) + b_2 \tag{A.2}$$

$$\frac{T_{t,in} - T_{t,out}}{T_{c,in}} = a_3 \left(Pr_T \left(\frac{T_{t,in} - T_{t,sol}}{T_{c,in}} + \frac{T_{t,in} - T_{bh}}{T_{c,in}} \right) \right) + b_3 \tag{A.3}$$

vel and vel_{max} refers to air velocity and was in this project neglected. a_1, b_1, a_2, b_2, a_3 and b_3 are constants found by using least square method. Pr_T is the pressure ratio. The pressure ratio is dependent on the mach number [1]. The mach number for the turbine, $M_{tip,T}$, is described in Equation A.4 and a correlation between the mach number and the pressure ratio can be described by Equation A.5

$$M_{tip,T} = \frac{\omega \times r_{tip,T}}{\sqrt{\gamma R_{exh} T_{c,in}}} \tag{A.4}$$

$$Pr_T = a_4 M_{tip,T}^2 + b_4 M_{tip,T} + c_4 \tag{A.5}$$

Where ω is the rotational speed of the turbo shaft, $r_{tip,T}$ is the radius of the impeller, R_{exh} is the gas constant and γ is the heat capacity ratio. a_4, b_4 and c_4 are constants found using curve fitting.

The model described above is to be used under stationary conditions, however with small adjustments it can also be used for transinent operation. During a load step can the wall temperatures be assumed to be unchanged for a while until changing towards the new stationary temperature. The speed however can be assumed to change instantly. So by using previous value on the wall temperatures together with the current pressure ratio can the turbine outlet temperature be determined even for transient condition.

B

Exhuast manifold temperatures, Method 2

In this model the exhaust manifold is seen as a straight pipe and corrections for the effects of heat transfer described in [27] combined with derivations done in [13] were used. Since the simplification that the exhaust manifold only consists of a straight pipe was made do the diameter and mass flow only consider a pipe coming from one cylinder. The fluid properties were set for a temperature mean value from measurements.

The Reynolds number was calculated as in Equation B.1.

$$Re = \frac{4\dot{m}}{\pi D \mu} \tag{B.1}$$

Where $\dot{m}$ is the fluid mass flow, D is the pipe inner diameter and μ is the viscosity at average bulk temperature.

The Prandtl number can be calculated with Equation B.2.

$$Pr = \frac{c_p \mu}{k} \tag{B.2}$$

Where c_p is the specific heat capacity if the exhaust gas, μ is the viscosity and k is the thermal conductivity.

Depending whether the flow is turbulent, laminar or in the transition area should a appropriate equation be chosen. For turbulent and transient flow can Equation B.3 be used.

$$Nu = 1.86 \left(RePr \frac{D}{L} \right)^{1/3} \left(\frac{\mu}{\mu_w} \right)^{0.14} \tag{B.3}$$

Where L is the pipe length and μ_w is a fluid property at wall temperature.

With this can the the heat transfer coefficient h be calculated with Equation B.4.

$$h = \frac{Nuk}{D} \tag{B.4}$$

The inlet temperature of the exhaust gas at exhaust manifold, $T_{m,in}$, will be known and the outlet temperature of the exhaust gas, $T_{t,in}$, will be guessed in the first iteration. The wall temperature was assumed to be evenly distributed and Equation B.5 which is derived in [13] will be used to determine the wall temperature. This is also compared to measurements done in the goods of the exhaust manifold.

$$T_w = \frac{T_{t,in} - T_{m,in}e^{\frac{-h\pi DL}{\dot{m}c_p}}}{1 - e^{\frac{-h\pi DL}{\dot{m}c_p}}} \tag{B.5}$$

A temperature mean value can be calculated with Equation B.6.

$$\Delta T_{ln} = \frac{\Delta T_1 - \Delta T_2}{ln(\Delta T_1 - \Delta T_2)} \tag{B.6}$$

where

$$\Delta T_1 = |T_w - T_{m,in}|, \quad \Delta T_2 = |T_w - T_{t,in}|$$

From this can the heat flow be calculated with Equation B.7 and from Equation B.8 can a new value of the pipe outlet temperature be decided. A new value of the wall temperature can be calculated and procedure is iterated until the temperature converges.

$$q = h\pi DL\Delta T_{ln} \tag{B.7}$$

$$q = \dot{m}c_p(T_{t,in} - T_{m,in}) \tag{B.8}$$

This approach is only suitable for steady state.

Bibliography

[1] Habib Aghaali and Hans-Erik Angstrom. Temperature estimation of turbocharger working fluids and walls under different engine loads and heat transfer conditions. In *SAE Technical Paper*. SAE International, 09 2013. doi: 10.4271/2013-24-0123. URL http://dx.doi.org/10.4271/2013-24-0123. Cited on pages 7 and 43.

[2] Habib Aghaali, Hans-Erik Ångström, and Jose R Serrano. Evaluation of different heat transfer conditions on an automotive turbocharger. *International Journal of engine research*, 16(2):137–151, 2015. Cited on page 7.

[3] Faghri Amir, Zhang Yuwen, and John Howell. *Advanced heat and mass transfer*. Global Digital Press, first edition, 2010. Cited on page 18.

[4] Nick Baines, Karl D. Wygant, and Antonis Dris. The analysis of heat transfer in automotive turbochargers. *Journal of Engineering for Gas Turbines and Power*, 132, 2010. Cited on page 6.

[5] Theodore L. Bergman and Adrienne S. Lavine. *Principles of heat and mass transfers*. John Wiley and Sons, seventh edition, 2012. Cited on page 10.

[6] Dieter E. Bohn, Norbert Moritz, and Michael Cano Wolff. Conjugate flow and heat transfer investigation of a turbo charger: Part ii - experimental results. *American Society of Mechanical Engineers, International Gas Turbine Institute, Turbo Expo (Publication) IGTI*, 3:723–729, 2003. Cited on page 7.

[7] R.D. Burke, C.D Copeland, T. Duda, and M.A Rayes-Belmonte. Lumped capacitance and three-dimensional computational fluid dynamics conjugate heat transfer modelingof an automotive turbocharger. *Journal of Engineering for Gas Turbines and Power*, 138, 2016. Cited on pages 1 and 7.

[8] Michael W. Casey and Thomas M. Feich. The efficiency of turbocharger compressors with diabatic flows. *Journal of engineering for gas turbines and power*, 132, 2010. Cited on page 8.

[9] Yunus A. Cengel, John M. Cimbala, Robert H Turner, and Mehmet Kanolu. *Fundamentals of thermal-fluid sciences*. McGraw-Hill, fourth edition, 2012. Cited on pages 4 and 5.

[10] Mickaël Cormerais, Pascal Chesse, and Jean-Francois Hetet. The analysis of heat transfer in automotive turbochargers. *Journal of Engineering for Gas Turbines and Power*, 132, 2010. Cited on page 7.

[11] M Deligant, P Podevin, and G Descombes. Experimental identification of turbocharger mechanical friction losses. *Energy*, 39:388–394, 2012. Cited on page 24.

[12] John C. Dixon. *The shock absorber handbook*. John Wiley and Sons Ltd, first edition, 2007. Cited on page 18.

[13] Lars Eriksson. Mean value models for exhaust system temperatures. *SAE Technical Paper*, 2002. Cited on pages 8, 13, 45, and 46.

[14] Lars Eriksson and Lars Nielsen. *Modeling and control of engines and drivelines*. John Wiley and Sons Ltd, first edition, 2014. Cited on pages 1, 3, 6, and 18.

[15] J.P. Holman. *Heat Transfer*. McGraw-Hill, tenth edition, 2010. Cited on page 10.

[16] lee kyu Hyun, Shim Chang-Yeul, and Kim Wan-Bum. Development of dual wall air gap exhaust system. *SAE Technical world congress*, 2000. Cited on page 8.

[17] Silvia Marelli, Guilio Marmorato, and Massismo Capobianco. Evaluation of heat transfer effects in small turbochargers by theoretical model and its experimental validation. *Energy*, 112:264–272, 2016. Cited on page 8.

[18] Silvia Marelli, Simone Gandolfi, and Massimo Capobianco. Heat transfer effect on performance map of a turbocharger turbine for automotive appliaton. In *Proc. WCX™ 17: SAE World Congress Experience*. SAE International, 2017. doi: 10.4271/2017-01-1036. Cited on page 8.

[19] Michael F. Modest. *Radiative heat transfer*. Elsevier Science, second edition, 2003. Cited on page 5.

[20] P. Olmeda, V. Doltz, F.J. Arnau, and M.A. Reyes-Belmonte. Determination of heat flows inside turbochargers by means of a one dimensional lumped model. *Mathematical and computer modelling*, 57:1847–1852, 2011. Cited on page 7.

[21] Francisco Payari, Pablo Omleda, Fransisco J. Arnau, Artem Dombrovsky, and Les Smith. External heat losses in small turbochargers: Model and experiments. *Energy*, 71:534–546, 2014. Cited on page 6.

[22] Alessandro Romagnoli and Martinez-Botas Ricardo. Heat transfer analysis in a turbocharger turbine: An experimental and computational evaluation. *Applied Thermal Engineering*, 38:58–77, 2011. Cited on page 7.

[23] J. R. Serrano, Tiseira A. Olmeda, P., L. M. Garcia-Cuevas, and A. Lefebvre. Importance of mechanical losses modeling in the performance prediction of radial turbochargers under pulsating flow conditions. *SAE Int. J.Engines*, 2013. Cited on page 20.

[24] José R. Serrano, Pablo Olmeda, Fransisco J. Arnau, Artem Dombrovsky, and Les Smith. Analysis and methodology to characterize heat transfer phenomena in automotive turbochargers. *Journal of engineering for gas turbines and power*, 137, 2015. Cited on page 7.

[25] José R. Serrano, Pablo Olmeda, Fransisco J. Arnau, and Miguel A. Reyes-Belmonte. A study on the internal convection in small turbochargers. proposal of heat transfer convective coefficients. *Applied thermal energy*, 89: 587–599, 2015. Cited on page 7.

[26] José Ramón Serrano, Pabla Olmeda, Fransisco J. Arnau, and Artem Dombrovsky. Turbocharger heat transfer and mechanical losses influence in predicting engines performance by using one-dimensional simulation codes. *Energy*, 86:204–218, 2015. Cited on page 7.

[27] Robert W Serth. *Process heat transfer, Principles and applications*. Academic press, 2007. Cited on pages 5 and 45.

[28] Borislav Sirakov and Michael Casey. Evaluation of heat transfer effects on turbocharger performance. *Journal of Turbomachinery*, 135, 2013. doi: 10. 1115/1.4006608. Cited on pages 6 and 8.

[29] Karl Storck, Matts Karlsson, Ingrid Andersson, Johan Renner, and Dan Loyd. *Formelsamling i termo-och fluiddynamik*. LiU-tryck, second edition, 2012. Cited on pages 4, 5, 10, and 29.

[30] Giovanni Tanda, Guilio Marmorato, and Massismo Capobianco. An experimental investigation of internal heat transfer in an automotive turbocharger compressor. *Applied energy*, 193:531–539, 2017. Cited on pages 6 and 8.

[31] Andrej Verem and Hiren Kerai. Physically based models for predicting exhaust temperatures in si engines. master thesis, Linköping University, 2016. Cited on page 20.